THE JOURNAL OF BIOLOGICAL CHEMISTRY VOL. 290, NO. 5, pp. 2938–2945, January 30, 2015

The Use of Carbohydrate Binding Modules (CBMs) to Monitor Changes in Fragmentation and Cellulose Fiber Surface Morphology during Cellulase- and Swollenin-induced Deconstruction of Lignocellulosic Substrates*

Received for publication, November 24, 2014, and in revised form, December 15, 2014 Published, JBC Papers in Press, December 19, 2014, DOI 10.1074/jbc.M114.627604

Keith Gourlay[‡], **Jinguang Hu**[‡], **Valdeir Arantes**[‡], **Merja Penttilä**[§], **and Jack N. Saddler**[‡1]

From the [‡]*Forest Products Biotechnology/Bioenergy Group, Department of Wood Science, Faculty of Forestry, University of British Columbia, Vancouver, British Columbia V6T 1Z4, Canada and the* [§]*VTT Technical Research Centre of Finland, Metallimiehenkuja 2 (Espoo), FI-02044 VTT, Finland*

Background: Fiber fragmentation is thought to occur at dislocations, which are potential targets for the non-hydrolytic protein, Swollenin.
Results: Changes in cellulose morphology within dislocations were assessed using fluorescent CBMs; Swollenin appeared to promote fragmentation at these sites.
Conclusion: Swollenin targets and disrupts cellulose at fiber dislocations.
Significance: Fragmentation is a key step in cellulose deconstruction and is enhanced by the actions of Swollenin.

Although the actions of many of the hydrolytic enzymes involved in cellulose hydrolysis are relatively well understood, the contributions that amorphogenesis-inducing proteins might contribute to cellulose deconstruction are still relatively undefined. Earlier work has shown that disruptive proteins, such as the non-hydrolytic non-oxidative protein Swollenin, can open up and disaggregate the less-ordered regions of lignocellulosic substrates. Within the cellulosic fraction, relatively disordered, amorphous regions known as dislocations are known to occur along the length of the fibers. It was postulated that Swollenin might act synergistically with hydrolytic enzymes to initiate biomass deconstruction within these dislocation regions. Carbohydrate binding modules (CBMs) that preferentially bind to cellulosic substructures were fluorescently labeled. They were imaged, using confocal microscopy, to assess the distribution of crystalline and amorphous cellulose at the fiber surface, as well as to track changes in surface morphology over the course of enzymatic hydrolysis and fiber fragmentation. Swollenin was shown to promote targeted disruption of the cellulosic structure at fiber dislocations.

The effective enzymatic hydrolysis of lignocellulosic substrates to fermentable sugars, for subsequent conversion to fuels and chemicals, could help the world transition from a fossil fuel-based economy to a global society that is more reliant upon renewable resources. To try to achieve the high sugar concentrations that can be obtained from sugar cane or corn, high-cellulosic solids reaction conditions are desirable as they reduce water consumption, enable the use of smaller reaction vessels, reduce distillation/separation costs for the desired end product and, consequently, reduce the overall capital and operating costs of the bioconversion process (1). However, high solids hydrolysis slurries have inherent issues with ease of mixing, pumpability, and mass transfer limitations during enzyme diffusion and adsorption to the substrate (2). Recent work has demonstrated that rapid fiber fragmentation at the very early stages of hydrolysis leads to a dramatic reduction in slurry viscosity, which alleviates some of the issues associated with high solids hydrolysis (2). It has been suggested that fiber fragmentation is primarily induced by the endoglucanase family of enzymes (3, 4), although other proteins present in the cellulolytic mixture, such as the more recently characterized oxidative enzymes (5, 6) and amorphogenesis-inducing proteins (7–9), have also been shown to contribute to the overall deconstruction process.

A considerable amount of earlier work has defined "cellulase mixtures" as a protein mixture containing predominantly endo- and exoglucanases and perhaps β-glucosidase. However, it is now largely recognized that, to achieve effective lignocellulose deconstruction of more realistic biomass substrates, the enzyme mixture must also contain accessory enzymes/proteins such as hemicellulases, lytic polysaccharide monooxygenases, and non-hydrolytic/non-oxidative proteins that have been shown to facilitate biomass degradation through the opening up of the lignocellulosic matrix (5, 7, 10, 11).

The non-hydrolytic non-oxidative proteins (also known as "disruptive" or "amorphogenesis-inducing" proteins) are of interest (7, 9, 12) due to their apparent ability to disrupt the structural matrix of biomass, consequently facilitating the subsequent depolymerization of the carbohydrate polymers by hydrolytic and oxidative enzymes (7). These disruptive proteins include examples from plants (Expansins) (13), bacteria (Expansin-like proteins (14, 15) and some carbohydrate binding modules (CBMs)[2] (16)), and fungi

* This work was supported by the Natural Sciences and Engineering Council of Canada (NSERC) and the Bioconversion Network.
[1] To whom correspondence should be addressed: Forest Products Biotechnology/ Bioenergy Group, Dept. of Wood Science, Faculty of Forestry, University of British Columbia, 2424 Main Mall, Vancouver, British Columbia V6T 1Z4, Canada. Tel.: 604-822-9741; E-mail: jack.saddler@ubc.ca.

[2] The abbreviations used are: CBM, carbohydrate binding module; FQA, fiber quality analyzer; AMCA-X, (6-((7-amino-4-methylcoumarin-3-acetyl)-amino)hexanoic acid; DMSO, dimethyl sulfoxide.

(Swollenin (8, 9, 12), Loosenin (17), and CBMs (18)). These proteins have also been shown to promote a variety of disruptive effects on cellulosic biomass, including filter paper dispersion, crystallinity reduction, particle size reduction, swelling of cotton fibers, and roughening of cotton fiber surface (7).

Swollenin, in particular, has been shown to effectively swell cotton fibers (9), disperse filter paper squares (12), roughen filter paper fibers (12), reduce the particle size of a number of model cellulosic substrates (12), enhance the accessibility of cotton fibers (19), and enhance hydrolysis (8, 20). Recent work has shown that Swollenin targets the less-ordered regions of the cellulose, rather than directly disrupting the more crystalline regions of the substrate (8, 19), and enhances the solubilization of the hemicellulosic fraction of steam-pretreated corn stover when it synergistically interacted with family 10 and 11 xylanases, promoting a 3-fold increase in xylose released by these hydrolases (8). It appears that, although Swollenin does to some extent enhance the disruption of well structured components of cellulosic substrates, its primary role is facilitating the disruption of the less-ordered regions of pretreated lignocellulosic substrates (8, 19).

It is possible that Swollenin targets the dislocations within lignocellulosic fibers, as these regions have been shown to be enriched in disordered/amorphous cellulose (21). Fiber dislocations (also called kinks, micro-compressions, irregularities, and slip planes (22)) have been observed in a range of plant species, including softwood, hemp, flax, and wheat (21, 23, 24). These dislocations are present in untreated biomass fibers and can also be induced during processing steps (25). Typically, the fiber structure within the dislocations contains surface features perpendicular to the direction of the microfibrils. Dislocations have also been shown to contain more amorphous cellulose with less order than the surrounding fiber, likely due to the distortion of the crystalline cellulose microfibrils (26), although other work has suggested that microfibrils continue through these dislocations (27). Earlier work has suggested that these dislocations within the fibers make up weak points that are rapidly hydrolyzed by cellulases (21).

In the work described here, we tried to better elucidate the potential role that Swollenin might play in fiber fragmentation by assessing various macroscopic fiber properties over the course of enzymatic hydrolysis of dissolving pulp and a range of pretreated substrates. Fiber quality analysis (FQA) was used to quantify the fiber length/particle size of cellulosic fibers, although the "settleability" of the pulp (*i.e.* how densely the pulp fibers compact after being allowed to settle in solution) was used as a secondary indicator of fiber length, as shorter fibers enable denser settling than longer ones.

To try to quantify possible changes at the microfibril level, a CBM adsorption technique (19) was also used. As described earlier by Boraston *et al.* (28), CBMs can be broadly categorized into the three types: Type A, which binds to well ordered (crystalline) substrates via a planar hydrophobic surface composed of tryptophan and tyrosine residues; Type B, which binds via a binding cleft to individual carbohydrate chains; and Type C, which binds via a binding pocket to chain ends and smaller carbohydrate molecules (28). The CBM adsorption technique used in the work described here compares the adsorption of a Type A and a Type B CBM with cellulose where the Type A CBM has been shown to preferentially adsorb to the more crystalline regions of the cellulose surface (29), whereas the Type B CBM preferentially binds to the more amorphous regions (30). Several previous studies have used CBMs with different specificities for crystalline and amorphous regions of the cellulose to try to reveal the differences in surface morphology between the surrounding fiber and the cellulose within fiber dislocations (21, 27, 31–33). However, no clear consensus was reached, with some Type A CBMs binding to dislocations (21, 31), whereas other Type A CBMs did not localize to these dislocations (32, 33). However, all of the Type B CBMs tested to date do appear to localize to fiber dislocations (31–33).

As described in more detail below, by monitoring fiber dimensions and assessing the binding profile of the fluorescently tagged CBMs on the fiber surface, we were able to show that Swollenin targeted the amorphous regions within the dislocations of cellulose fibers, promoting fiber fragmentation at these dislocations.

EXPERIMENTAL PROCEDURES

Proteins—A cellobiohydrolase (CEL7A), an endoglucanase (CEL5A), and an endoxylanase (XYN10A) were purified as described previously (10). Swollenin was expressed in *Trichoderma reesei*, under the *cbh1* promoter with a C-terminal His_6 tag, and purified using immobilized metal ion affinity chromatography followed by anion exchange chromatography (DEAE-Sepharose). The procedure used previously with CEL61A (34) was followed. CBM2a from *Cellulomonas fimi* was purified from *Escherichia coli* using the following procedure (35). Cells were grown at 37 °C in Terrific Broth to A_{280} ~2.0 and then induced with 0.2 mM isopropyl-β-D-1-thiogalactopyranoside (Sigma-Aldrich) and incubated for an additional 24–32 h at 30 °C. Cells were harvested by centrifugation, and the pellet was then used immediately for purification or frozen for future use. Cells were lysed by shaking in 5 ml of BugBuster (EMD Millipore) per gram of cell paste supplemented with Benzonase nuclease (EMD Millipore) for 20 min at room temperature. Lysed cells were clarified by centrifugation, and the clarified extract was added to Avicel (15 g of Avicel per liter of original cell culture) and incubated for 1 h at room temperature or overnight at 4 °C. The slurry was then filtered and washed three times with 1 M sodium chloride in 50 mM potassium phosphate (pH 7.0) and three times with 50 mM potassium phosphate (pH 7.0) and then eluted by incubating the cellulose paste with 6 M guanidine hydrochloride for 30 min at room temperature before filtering. All subsequent steps were performed on ice to prevent precipitation. The CBM2a solution in 6 M guanidine hydrochloride was concentrated to ~0.10 volume over an Amicon (EMD Millipore) ultrafiltration apparatus using a 10-kDa polysulfone membrane (EMD Millipore). The concentrated solution was then centrifuged to remove fines and precipitated material and then slowly diluted ~20 times with 1 mM ice-cold potassium phosphate (pH 7.0) to refold the CBM. This solution was then concentrated again and rediluted with 1 mM ice-cold potassium phosphate (pH 7.0). Finally, CBM2a was desalted into 50 mM potassium phosphate (pH 7.0). CBM44 from *Clostridium thermocellum* was purchased from NZYTech (CR0049, Lisbon, Portugal).

Fibers—Hardwood-derived dissolving pulp was provided by Tembec (Montréal, Canada). Steam-pretreated and ethanol-organosolv-pretreated corn stover, poplar, and lodgepole pine were pretreated at near optimal conditions as described previously (36, 37).

Enzyme Treatments—Dissolving pulp (6 g of dry weight) was weighed into 250-ml Erlenmeyer flasks and hydrolyzed in 120 ml of 50 mM sodium acetate buffer (pH 5.0) using an enzyme loading of 13 mg of Celluclast 1.5L (Novozymes, Bagsværd, Denmark) per gram of pulp (dry weight), supplemented with 5 cellobiase units (equivalent to 2 mg of β-glucosidase) per gram of pulp (dry weight). Celluclast 1.5L contains a mixture of fungal hydrolytic enzymes that is predominantly composed of two cellobiohydrolases, two endoglucanases, and lesser amounts of other cellulases and various accessory enzymes (10). Flasks were stoppered and incubated in a shaking incubator at 50 °C. After the desired elapsed time, flasks were transferred to a hot water bath set to 100 °C and incubated for 15 min. Glucose release was measured by the glucose oxidase assay (38, 39). For the 0-h time point, the buffer was added to the pulp, and the sample was transferred to the hot water bath prior to adding enzyme. As the temperature increased past 60 °C, enzyme was added. This was done to get very rapid inactivation of the enzymes in the 0-h sample. Hydrolyzed pulps were then filtered, washed three times with water and then incubated with protease. A protease solution was prepared by diluting proteinase from *Aspergillus melleus* (Sigma) to a concentration of 1 unit/ml in 50 mM potassium phosphate buffer, pH 7, and incubated overnight at 37 °C. After protease treatment, samples were filtered, washed three times with 100 ml of 1 M sodium chloride in 50 mM potassium phosphate (pH 7.0), washed three times with 100 ml of 50 mM potassium phosphate (pH 7.0), and washed three times with 100 ml of nanopure water. Removal of protein from the pulp was confirmed by the ninhydrin assay as described previously (data not shown) (40).

For pulps treated with isolated enzymes (CEL7A, CEL5A, XYN10A, and Swollenin), the reactions were carried out in 2-ml screw cap tubes containing 2 mg (dry weight) of dissolving pulp in 1.5 ml of 50 mM sodium acetate (pH 5.0) with 50 μg of enzyme per mg of pulp. Samples were incubated overnight with shaking at 50 °C. Prior to FQA, the samples were heat inactivated at 100 °C for 10 min.

FQA and Settleability—Changes in fiber length were determined using a high-resolution fiber quality analyzer (LDA02, OpTest Equipment, Inc., Hawkesbury, Ontario, Canada) as described previously (37). All samples were run in at least triplicate. The number of fibers counted per sample was 20,000. The ranges of fiber length and fiber width measured were 0.05–10.00 mm and 7–60 μm, respectively. Settleability was visualized by weighing out 10 mg (dry weight) of hydrolyzed pulp and then staining overnight in 1 ml of 0.5 mg/ml Direct Orange (Pontamine Fast Orange 6RN, lot number 814071, Pylam Products Co. Inc., Garden City, NY) in PBS buffer at 70 °C in a shaking incubator. Samples were then centrifuged, and the liquid was exchanged 10 times with water to remove any unbound dye. Dyed fibers were then allowed to gravity-settle in upright 1.5-ml Eppendorf tubes for 2 days.

CBM Adsorption—CBM adsorption was carried out as described previously (19). Briefly, 250 μg of CBM (as determined by absorption at 280 nm) was added to 2.5 mg (dry weight) of pulp in 1 ml of 50 mM potassium phosphate (pH 7.0). Samples were incubated for 60 min at 20 °C in a FinePCR Combi-SV12 hybridization incubator at 30 rpm and then centrifuged at 16,000 × *g* for 10 min in a benchtop centrifuge. The amount of CBM bound to the cotton was calculated by measuring the absorbance of the supernatant at 280 nm and determining the concentration of the residual CBM in the supernatant using the calculated molar extinction coefficients of 27,625 and 27,365 $M^{-1}cm^{-1}$ for CBM2a and CBM44, respectively (29). The amount of CBM bound to the cotton was calculated by subtracting the amount of the residual CBM in the supernatant from the original amount of CBM added to the sample.

Fluorescent Tagging of CBMs—To tag the CBMs, each CBM was made up to 5 mg/ml in 1 ml of 0.1 M sodium bicarbonate buffer, pH 8.3. A 10:1 ratio of protein to dye was used for tagging. Specifically, 0.5 mg of dye (6-((7-amino-4-methylcoumarin-3-acetyl)amino)-hexanoic acid, (AMCA-X, Life Technologies) for CBM2a and Oregon Green 514 (Life Technologies) for CBM44) was dissolved in 50 μl of dimethyl sulfoxide (DMSO, Sigma Aldrich). While stirring/vortexing the protein solution (~5 mg in 1 ml), the 50-μl AMCA or Oregon Green 514 solution in DMSO was added and incubated at room temperature with continuous shaking for 1 h. The dyed CBMs were then desalted into 50 mM potassium phosphate, pH 7.0. It should be noted that the binding of CBM44 was significantly reduced (to ~10% of original capacity) after tagging, suggesting that some of the CBMs were tagged at or near the binding cleft, inhibiting the binding of the CBM. However, it was apparent that not all CBM44 molecules were inhibited in their binding, as confocal microscopy was still able to detect these CBMs bound to the cellulose fibers.

X-ray Diffraction—Cellulose crystallinity index was measured by x-ray diffraction as described in Nishiyama *et al.* (41). Briefly, pulp samples were hydrolyzed, washed, filtered, and freeze-dried, and then mounted onto a zero-background plate. The data were collected with a Bruker D8-Advance powder x-ray diffractometer. Bruker TOPAS version 4.2 was used to model the percentage of crystallinity, and Nishiyama's cellulose 1β was used to model cellulose. The percentage of cellulose crystallinity was calculated as: 100 × (crystalline area/total area), where the total area = crystalline area + amorphous area.

Confocal Microscopy—Confocal microscope imaging was performed using an inverted Zeiss Axiovert LSM 5 confocal microscope equipped with epifluorescence, Nomarski optics, and LSM 5 Pascal software. Image acquisition and analysis were done with the LSM 5 Pascal volume-rendering software. Images were opened with the GNU Image Manipulation Program (GIMP) version 2.8. To produce the overlaid image, the colored pixels were extracted from both images, and a minimum threshold pixel intensity was set to filter out weakly colored regions. The remaining pixels were then saturated and overlaid on top of the original SEM image.

RESULTS AND DISCUSSION

Quantifying Fiber Properties during Hydrolysis—We initially wanted to quantify the possible influence of hydrolytic enzymes

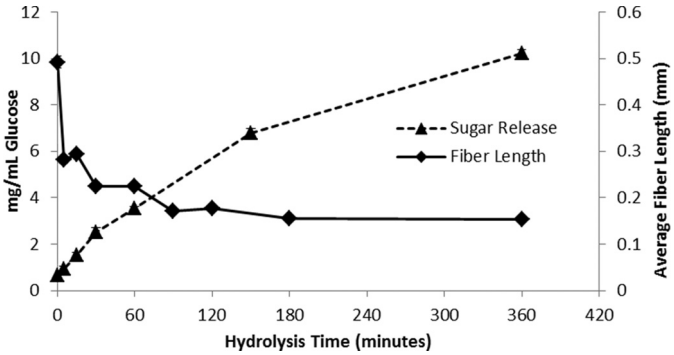

FIGURE 1. **Sugar release and average fiber length during enzymatic hydrolysis of dissolving pulp using 15 mg of enzyme/g of glucan.** All reactions were performed in triplicate, and *error bars* represent mean ± S.D.

on fiber fragmentation and cellulose surface morphology using a unique dual-probe CBM adsorption technique. Previous work had shown that enzyme-mediated fiber cutting seems to predominantly occur at the disordered regions of cellulosic fibers known as dislocations (21, 42). In the work described here, we used a fiber quality analyzer, which calculates fiber length, width, and size distribution measurements via high-throughput image analysis of fiber samples, to track any fiber changes over the course of hydrolysis of a hardwood dissolving pulp. Enzymatic hydrolysis was carried out on 6-g samples of dissolving pulp in 150-ml flasks using 13 mg/g of Celluclast 1.5L supplemented with 2 mg/g of β-glucosidase as described under "Enzyme Treatments" (see "Experimental Procedures"). A dramatic reduction in fiber length was observed (Fig. 1) at the very early stages of hydrolysis, with an almost 50% reduction in mean fiber length occurring within 5 min of cellulase addition. A further reduction in fiber length was observed between 60 and 90 min, with no further reductions in fiber length observed after this time.

The trends observed by FQA analyses seemed to correlate well with the observed settleability of the hydrolyzed pulps (Fig. 2). To quantify pulp settleability, equal masses of pulps from each hydrolysis time point were dyed with Direct Orange dye, washed to remove any background color, and subsequently allowed to settle in water in a 1.5-ml Eppendorf tube. Settleability also happened in a stepwise fashion, first occurring after just 5 min of hydrolysis with little change from 5 to 60 min (Fig. 2). However, between 60 and 90 min, the pulp settleability dropped further to a final steady level, remaining relatively constant from 90 min onwards.

The observed, very early, reduction in fiber length during hydrolysis was in agreement with recent rheology work that also showed a rapid (within 5 min) reduction in viscosity during Solka-Floc hydrolysis (43). As the hydrolysis rate remained more or less constant during this time, this suggested that, at least under the low-consistency conditions used here (*i.e.* less than ~5% solids loading), the observed changes in fiber length of the substrate did not significantly influence the rate of hydrolysis. This was consistent with earlier work, which showed that changes in the initial fiber length of organosolv-pretreated softwoods did not appear to influence the rate of low-consistency enzymatic hydrolysis (44). During the enzymatic hydrolysis of dissolving pulp, a plateau in settleability was observed after 90 min of hydrolysis, which agreed with the plateau in fiber length reduction detected by FQA. It is possible that there are two classes of fiber dislocations, one that is highly disrupted and is cleaved within the first 5 min of hydrolysis (major dislocations) and a second that is more recalcitrant to cleavage and is cleaved between 60 and 90 min (minor dislocations). This classification of dislocations into major and minor dislocations is not meant to describe the abundance of each type of dislocation, but rather to describe the intensity or severity of the dislocations.

To determine whether the reduction in fiber length over the course of hydrolysis corresponded with specific changes in the surface morphology of the cellulose, a previously described cellulose substructure-specific CBM technique was used (19). A Type B CBM (CBM44), which contains a cleft-shaped binding site that preferentially binds to amorphous regions of cellulose (30), was used as a probe to determine the amount of accessible amorphous cellulose, whereas a Type A CBM (CBM2a), with a planar, hydrophobic binding face that preferentially binds to crystalline cellulose regions (29), was used as a probe to determine the amount of accessible crystalline cellulose on the dissolving pulp fibers. The amount of each CBM bound to the variably hydrolyzed dissolving pulp over the course of 6 h was used to determine the relative amounts of accessible amorphous and accessible crystalline cellulose (Fig. 3). A rapid and dramatic reduction (50%) in the amount of accessible amorphous cellulose occurred within the first 5–15 min of hydrolysis. After this initial drop, the amount of accessible amorphous cellulose remained constant for the remainder of the course of hydrolysis. Although the amount of accessible crystalline cellulose, as determined by the adsorption of CBM2a, also declined, it was at a slower rate and to a lesser extent than the decline in accessible amorphous cellulose (Fig. 3).

Although the amount of amorphous binding CBM that had adsorbed to the substrate dropped dramatically within the first 5–15 min of hydrolysis, this reduction occurred when only 2.0% (± 0.3%) of the original substrate had been solubilized (calculated from the data used to generate Fig. 1). This implied that there was a small amount of highly accessible, rapidly hydrolyzed amorphous cellulose present in the pulp fibers. Previous work (21) has shown that the dislocations where fragmentation occurs are enriched in amorphous cellulose. Thus, it is likely that the amorphous cellulose within the fiber dislocations is the target for this rapid initial hydrolysis, leading to the observed reductions in both the average fiber length and accessible amorphous cellulose. Recent work by Gao *et al.* (45) has also suggested this type of mechanism.

We next carried out x-ray diffraction of the variably hydrolyzed dissolving pulps to see whether the observed changes in the surface morphology of the hydrolyzed samples correlated with changes in the crystallinity of the samples. The bulk crystallinity of the pulp samples appeared to increase slightly over the first 5 min of hydrolysis, after which it remained relatively constant for the remainder of the hydrolysis reaction (Fig. 4). The slight increase in cellulose crystallinity that was observed over the first 5 min of hydrolysis seemed to complement the CBM adsorption data. This again suggested that there was a small amount of accessible amorphous cellulose at the surface of the cellulosic

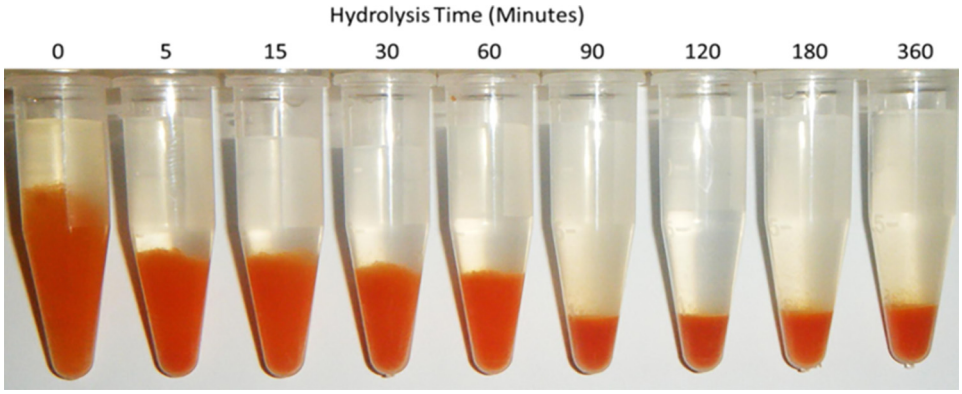

FIGURE 2. Dissolving pulp was hydrolyzed at 15 mg of enzyme/g of glucan for various lengths of time. Equal masses of dissolving pulp were then weighed out, stained with Direct Orange dye to enhance visibility, washed thoroughly, and allowed to settle overnight.

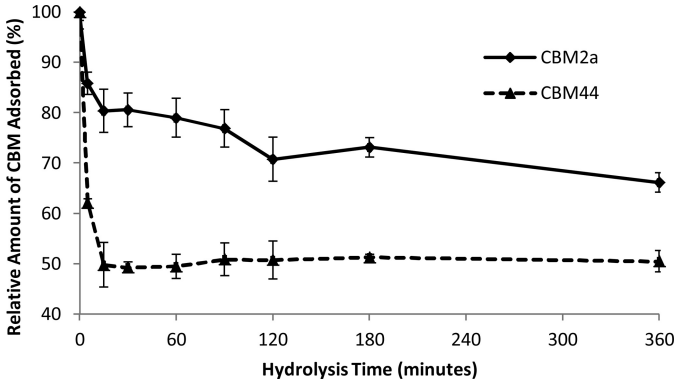

FIGURE 3. **Relative amount of CBM adsorbed to dissolving pulp over the course of hydrolysis.** CBM2a binding indicates accessible crystalline cellulose, whereas CBM44 binding represents accessible amorphous cellulose. Values are relative to the initial amount of CBM adsorbed to the unhydrolyzed pulp. All reactions were performed in triplicate, and *error bars* represent mean ± S.D.

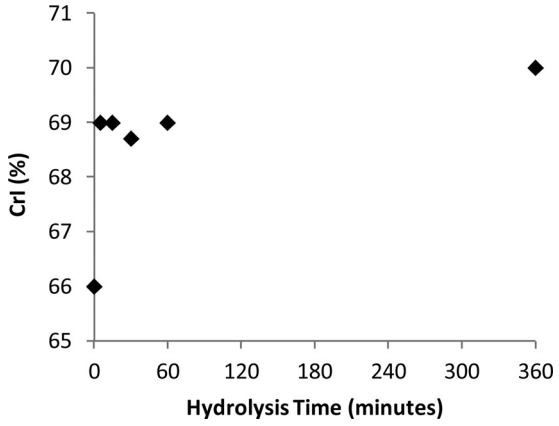

FIGURE 4. **Crystallinity index (*CrI*) of dissolving pulp over the course of enzymatic hydrolysis as determined by x-ray diffraction.**

fibers, which was rapidly hydrolyzed during the first few minutes of hydrolysis. After this initial removal of the highly accessible amorphous cellulose, the crystallinity of the sample did not change, implying that both the amorphous and the crystalline regions were hydrolyzed simultaneously. These observations are consistent with a model where initial fiber fragmentation might be followed by a "layer by layer," "peeling," or "shaving" mechanism of hydrolysis, where layers of cellulose containing both the amorphous and the crystalline regions are hydrolyzed together (46, 47).

Confocal Imaging of CBM Distribution—To try to determine whether the amorphous cellulose component of the dissolving pulp fibers prior to hydrolysis was distributed evenly across the fiber surface or localized to specific features of the fibers, the amorphous binding and crystalline binding CBMs were each tagged with a different amine-reactive probe. Specifically, CBM44 was tagged with Oregon Green 514, and CBM2a was tagged with a blue probe, AMCA-X. When the tagged CBMs were simultaneously incubated with dissolving pulp and imaged on a confocal microscope (Fig. 5), the CBM2a and CBM44 were found to have distinct binding patterns, with the amorphous binding CBM (CBM44) preferentially localizing to the fiber dislocations, whereas the crystalline binding CBM (CBM2a) was more generally bound to the smoother regions of the fiber surface (Fig. 5). It is important to note that the patterns observed for each CBM were dependent on the gain settings used during image acquisition. For example, if gain settings were maximized, then both CBMs appeared to bind to the entire surface of the fiber. It was only by lowering the gain settings that changes in the distributions of the CBMs on the fiber surface became apparent. Thus, although both CBMs do bind to the entire surface of the fiber, the binding density (amount bound per unit area) of each CBM exhibited distinct patterns. In other words, both CBMs bound throughout the surface of the fiber, but CBM44 had a higher binding density at dislocations, whereas CBM2a had a higher binding density along the more organized and well structured surfaces of the fibers.

In earlier work, Type B CBMs, including members of families CBM4, CBM6, and CBM28, were shown to preferentially bind to fiber dislocations (32, 33), agreeing with the preferential adsorption of CBM44 to the fiber dislocations observed here, whereas related work using bacterial Type A CBMs (such as CBM2a) showed that these CBMs do not preferentially bind to these types of dislocations. For example, two Type A family 3 CBMs from the cellulosome complexes of *Clostridium josui* and *C. thermocellum* did not preferentially bind to dislocations (28). The results reported here are most similar to those of Kawakubo *et al.* (32), who found that the Type B CBM28 preferentially bound to dislocations, whereas the Type A CBM3 from *C. josui* did not. However, Fox *et al.* (48) showed that a CBM3a similar to that used by Kawakubo *et al.* (32) was a particularly promiscuous CBM as it bound to both the amorphous and the crystalline regions of cellulose. Thus, it was likely that

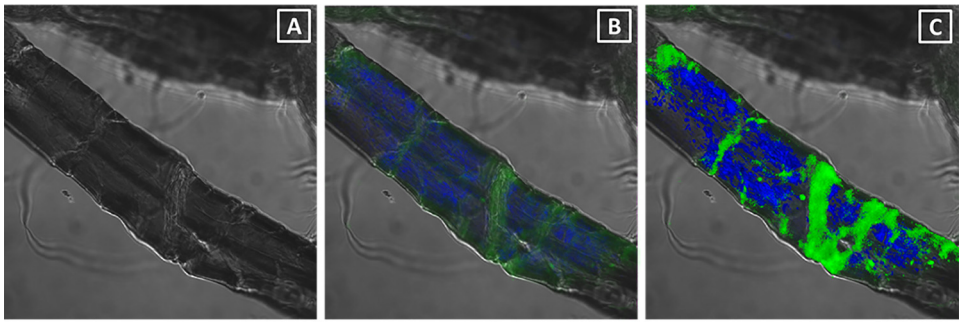

FIGURE 5. *A* and *B*, a representative dissolving pulp fiber shown with (*A*) and without (*B*) the fluorescence distribution from fluorescently tagged CBMs. *C*, the enhanced picture shows the clear contrast of the binding profile of different family CBMs. The *blue color* represents emission from CBM2a, whereas the *green color* represents emission from CBM44. A major dislocation can be seen toward the right of the fiber, whereas a minor dislocation can be seen toward the left.

the *C. thermocellum* CBM2a used in the work reported here was a better choice as a probe for crystalline cellulose.

The outliers in the adsorption profile of the CBMs are the fungal family 1 CBMs (21, 31, 49) as these small (~4 kDa, as compared with 27 kDa for CBM44 and 11 kDa for CBM2a (30, 35)) Type A fungal enzyme-derived CBMs are known to preferentially bind to dislocations. These CBMs, which have the highest binding order parameters of all CBMs studied to date (indicating a high preference for crystalline cellulose (48)), appear to localize at dislocations. It is possible that the small sizes of these CBMs play a role in their binding to dislocations due to adsorption/entrapment within nanoscopic pores in the surface of dislocations that are two small for the larger bacterial CBMs. However, the presence of these putative pores has yet to been confirmed, and it is possible that the unusual binding of these family 1 CBMs to dislocations could stem from a specific structural element of this CBM. These apparently contradictory observations (preferential binding to dislocations and high binding order parameter (48)) warrant further investigation into both the true specificity of this CBM, as well as the techniques used to assess preferential binding to amorphous or crystalline cellulose.

Effects of Swollenin on Dissolving Pulp—As previous work had shown that Swollenin could disrupt the less-ordered regions of biomass (8), we next wanted to see whether Swollenin could aid in initial cellulose hydrolysis by promoting fiber fragmentation at dislocations. Swollenin-induced fiber fragmentation was compared with the fragmenting activity of an isolated cellobiohydrolase (CEL7A), an endoglucanase (CEL5A), and a xylanase, as well as a BSA control. When these enzymes were added individually, only the endoglucanase was able to fragment the fibers to any great extent (Fig. 6). This was anticipated as earlier work (4, 21) had shown that fiber fragmentation was primarily induced by endoglucanases. Despite its lack of discernible hydrolytic activity, Swollenin was able to promote fragmentation of dissolving pulp fibers, although to a lesser extent than did Cel5A (Fig. 6). However, when Swollenin was incubated with a range of pretreated lignocellulosic substrates, including steam-pretreated and organosolv-pretreated corn stover, poplar, and lodgepole pine, no reduction in fiber length was observed (Fig. 7). Thus, it is probable that other substrate factors influence the effectiveness of Swollenin-induced fiber fragmentation, such as the amount and type of residual hemicellulose and lignin and the occurrence and role of lignin-carbohydrate complexes.

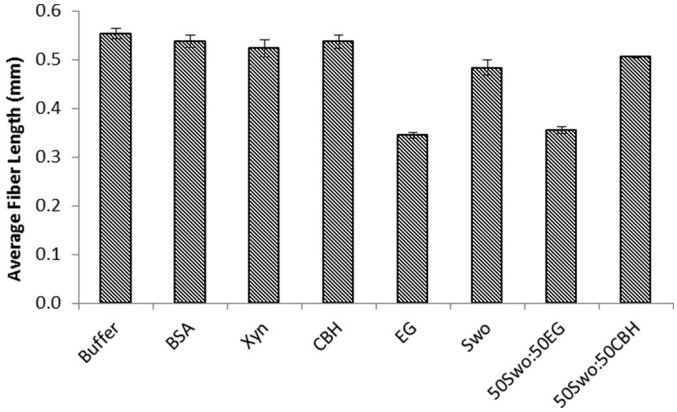

FIGURE 6. **Average fiber length of dissolving pulp fibers treated with individual enzymes and binary enzyme combinations.** The abbreviations used are: *Xyn*, xylanase; *CBH*, cellobiohydrolase ; *EG*, endoglucanase; *Swo*, Swollenin. All samples were run in triplicate, and *error bars* represent mean ± S.D.

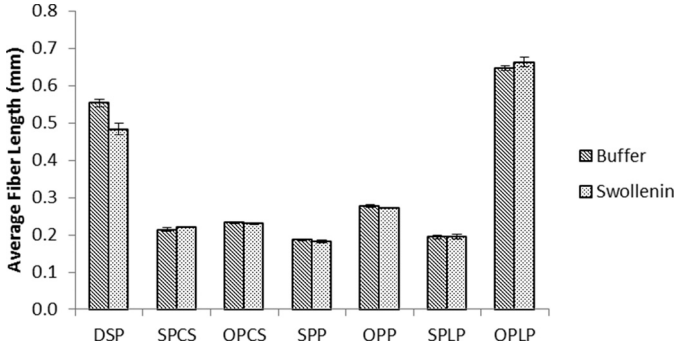

FIGURE 7. **Average fiber length of various pretreated lignocellulosic pulps after treatment with either buffer or Swollenin.** The abbreviations used are: *DSP*, dissolving pulp; *SPCS*, steam-pretreated corn stover; *OPCS*, organosolv-pretreated corn stover; *SPP*, steam-pretreated poplar; *OPP*, organosolv-pretreated poplar; *SPLP*, steam-pretreated lodgepole pine; *OPLP*, organosolv-pretreated lodgepole pine. All samples were run in triplicate, and *error bars* represent mean ± S.D.

As previous work had suggested that Swollenin can weaken hydrogen bonding within amorphous regions of cellulose and hemicellulose (8, 9, 12), it is possible that Swollenin promotes fiber fragmentation by weakening hydrogen bonds and enhancing slippage between adjacent chains within fiber dislocations. This weakening of hydrogen bonding and chain slippage might be sufficient to cause fragmentation within certain severe dislocations, but not within the less severe dislocations.

In summary, when substrate changes occurring during hydrolysis were monitored, using the FQA and CBM adsorption tech-

niques, fiber fragmentation was found to occur via a "two-step" process, with the first stage fiber length reduction occurring within minutes and the second occurring over 60–90 min. The solubilization of the small amount of more accessible amorphous cellulose that is hydrolyzed within the first few minutes, although only constituting about 2% of the initial cellulose, seems to play a key role in facilitating fiber fragmentation. Confocal microscopy showed that this amorphous cellulose was concentrated within fiber dislocations, implying that the rapid reduction in fiber length and reduction in binding of the amorphous binding CBM was primarily due to hydrolysis of the amorphous cellulose within fiber dislocations. When various combinations of monocomponent enzymes/proteins were added to dissolving pulp and pretreated lignocellulosic substrates, Swollenin, which is a non-hydrolytic non-oxidative protein, was also shown to promote fiber fragmentation by targeting the amorphous cellulose within fiber dislocations. It is possible that Swollenin may function by enhancing hydrogen bond disruption, resulting in slippage between cell wall components and the consequential disruption/separation at fiber dislocations.

Acknowledgments—We thank Novozymes, Bagsværd, Denmark for supplying enzymes and Martina Andberg and Markku Saloheimo of VTT for Swollenin.

REFERENCES

1. Huang, W.-D., and Zhang, Y.-H. P. (2011) Analysis of biofuels production from sugar based on three criteria: thermodynamics, bioenergetics, and product separation. *Energy Environ. Sci.* **4,** 784–792
2. Kristensen, J. B., Felby, C., and Jørgensen, H. (2009) Yield-determining factors in high-solids enzymatic hydrolysis of lignocellulose. *Biotechnol. Biofuels.* **2,** 11
3. Halliwell, G., and Riaz, M. (1970) The formation of short fibres from native cellulose by components of *Trichoderma koningii* cellulase. *Biochem J.* **116,** 35–42.
4. Walker, L. P., Wilson, D. B., Irvin, D. C., McQuire, C., and Price, M. (1992) Fragmentation of cellulose by the major *Thermomonospora fusca* cellulases, *Trichoderma reesei* CBHI, and their mixtures. *Biotechnol. Bioeng.* **40,** 1019–1026
5. Harris, P. V., Welner, D., McFarland, K. C., Re, E., Navarro Poulsen, J.-C., Brown, K., Salbo, R., Ding, H., Vlasenko, E., Merino, S., Xu, F., Cherry, J., Larsen, S., and Lo Leggio, L. (2010) Stimulation of lignocellulosic biomass hydrolysis by proteins of glycoside hydrolase family 61: structure and function of a large, enigmatic family. *Biochemistry (Mosc.)* 49, 3305–3316
6. Quinlan, R. J., Sweeney, M. D., Lo Leggio, L., Otten, H., Poulsen, J.-C. N., Johansen, K. S., Krogh, K. B. R. M., Jørgensen, C. I., Tovborg, M., Anthonsen, A., Tryfona, T., Walter, C. P., Dupree, P., Xu, F., Davies, G. J., and Walton, P. H. (2011) Insights into the oxidative degradation of cellulose by a copper metalloenzyme that exploits biomass components. *Proc. Natl. Acad. Sci.* **108,** 15079–15084
7. Arantes, V., and Saddler, J. N. (2010) Access to cellulose limits the efficiency of enzymatic hydrolysis: the role of amorphogenesis. *Biotechnol. Biofuels.* **3,** 4
8. Gourlay, K., Hu, J., Arantes, V., Andberg, M., Saloheimo, M., Penttilä, M., and Saddler, J. (2013) Swollenin aids in the amorphogenesis step during the enzymatic hydrolysis of pretreated biomass. *Bioresour. Technol.* **142,** 498–503
9. Saloheimo, M., Paloheimo, M., Hakola, S., Pere, J., Swanson, B., Nyyssönen, E., Bhatia, A., Ward, M., and Penttilä, M. (2002) Swollenin, a *Trichoderma reesei* protein with sequence similarity to the plant expansins, exhibits disruption activity on cellulosic materials. *Eur. J. Biochem.* **269,** 4202–4211
10. Hu, J., Arantes, V., and Saddler, J. N. (2011) The enhancement of enzymatic hydrolysis of lignocellulosic substrates by the addition of accessory enzymes such as xylanase: is it an additive or synergistic effect? *Biotechnol. Biofuels.* **4,** 36
11. Hu, J., Arantes, V., Pribowo, A., Gourlay, K., and Saddler, J. N. (2014) Substrate factors that influence the synergistic interaction of AA9 and cellulases during the enzymatic hydrolysis of biomass. *Energy Environ. Sci.* **7,** 2308–2315
12. Jäger, G., Girfoglio, M., Dollo, F., Rinaldi, R., Bongard, H., Commandeur, U., Fischer, R., Spiess, A. C., and Büchs, J. (2011) How recombinant swollenin from *Kluyveromyces lactis* affects cellulosic substrates and accelerates their hydrolysis. *Biotechnol. Biofuels.* **4,** 33
13. Cosgrove, D. J. (2000) Loosening of plant cell walls by expansins. *Nature* **407,** 321–326
14. Kerff, F., Amoroso, A., Herman, R., Sauvage, E., Petrella, S., Filée, P., Charlier, P., Joris, B., Tabuchi, A., Nikolaidis, N., and Cosgrove, D. J. (2008) Crystal structure and activity of *Bacillus subtilis* YoaJ (EXLX1), a bacterial expansin that promotes root colonization. *Proc. Natl. Acad. Sci. U.S.A.* **105,** 16876–16881
15. Lee, H. J., Lee, S., Ko, H.-J., Kim, K. H., and Choi, I.-G. (2010) An expansin-like protein from *Hahella chejuensis* binds cellulose and enhances cellulase activity. *Mol. Cells.* **29,** 379–385
16. Din, N., Gilkes, N. R., Tekant, B., Miller, R. C., Warren, R. A. J., and Kilburn, D. G. (1991) Non-hydrolytic disruption of cellulose fibres by the binding domain of a bacterial cellulase. *Nat. Biotechnol.* **9,** 1096–1099
17. Quiroz-Castañeda, R. E., Martínez-Anaya, C., Cuervo-Soto, L. I., Segovia, L., and Folch-Mallol, J. L. (2011) Loosenin, a novel protein with cellulose-disrupting activity from Bjerkandera adusta. *Microb. Cell Fact.* **10,** 8
18. Lee, I., Evans, B. R., and Woodward, J. (2000) The mechanism of cellulase action on cotton fibers: evidence from atomic force microscopy. *Ultramicroscopy.* **82,** 213–221
19. Gourlay, K., Arantes, V., and Saddler, J. N. (2012) Use of substructure-specific carbohydrate binding modules to track changes in cellulose accessibility and surface morphology during the amorphogenesis step of enzymatic hydrolysis. *Biotechnol. Biofuels.* **5,** 51
20. Kang, K., Wang, S., Lai, G., Liu, G., and Xing, M. (2013) Characterization of a novel swollenin from *Penicillium oxalicum* in facilitating enzymatic saccharification of cellulose. *BMC Biotechnol.* **13,** 42
21. Thygesen, L. G., Hidayat, B. J., Johansen, K. S., and Felby, C. (2011) Role of supramolecular cellulose structures in enzymatic hydrolysis of plant cell walls. *J. Ind. Microbiol. Biotechnol.* **38,** 975–983
22. Nyholm, K, Ander, P., Bardage, S., and Daniel, G. (2001) Dislocations in pulp fibres — their origin, characteristics and importance — a review. *Nord. Pulp Pap. Res. J.* **16,** 376–384
23. Thygesen, L. G., Eder, M., and Burgert, I. (2007) Dislocations in single hemp fibres: investigations into the relationship of structural distortions and tensile properties at the cell wall level. *J. Mater. Sci.* **42,** 558–564
24. Baley, C. (2004) Influence of kink bands on the tensile strength of flax fibers. *J. Mater. Sci.* **39,** 331–334
25. Eder, M., Terziev, N., Daniel, G., and Burgert, I. (2007) The effect of (induced) dislocations on the tensile properties of individual Norway spruce fibres. *Holzforschung.* **62,** 77–81
26. Ander, P., Hildén, L., and Daniel, G. (2008) Cleavage of softwood kraft pulp fibres by HCl and cellulases. *BioResources.* **3,** 477–490
27. Hidayat, B. J., Felby, C., Johansen, K. S., and Thygesen, L. G. (2012) Cellulose is not just cellulose: a review of dislocations as reactive sites in the enzymatic hydrolysis of cellulose microfibrils. *Cellulose.* **19,** 1481–1493
28. Boraston, A. B., Bolam, D. N., Gilbert, H. J., and Davies, G. J. (2004) Carbohydrate-binding modules: fine-tuning polysaccharide recognition. *Biochem. J.* **382,** 769–781
29. McLean, B. W., Boraston, A. B., Brouwer, D., Sanaie, N., Fyfe, C. A., Warren, R. A. J., Kilburn, D. G., and Haynes, C. A. (2002) Carbohydrate-binding modules recognize fine substructures of cellulose. *J. Biol. Chem.* **277,** 50245–50254
30. Najmudin, S., Guerreiro, C. I. P. D., Carvalho, A. L., Prates, J. A. M., Correia, M. A. S., Alves, V. D., Ferreira, L. M. A., Romão, M. J., Gilbert, H. J., Bolam, D. N., and Fontes, C. M. G. A. (2006) Xyloglucan is recognized by carbohydrate-binding modules that interact with β-glucan chains. *J. Biol. Chem.* **281,** 8815–8828
31. Filonova, L., Kallas, A. M., Greffe, L., Johansson, G., Teeri, T. T., and

Daniel, G. (2007) Analysis of the surfaces of wood tissues and pulp fibers using carbohydrate-binding modules specific for crystalline cellulose and mannan. *Biomacromolecules.* **8,** 91–97
32. Kawakubo, T., Karita, S., Araki, Y., Watanabe, S., Oyadomari, M., Takada, R., Tanaka, F., Abe, K., Watanabe, T., Honda, Y., and Watanabe, T. (2010) Analysis of exposed cellulose surfaces in pretreated wood biomass using carbohydrate-binding module (CBM)-cyan fluorescent protein (CFP). *Biotechnol. Bioeng.* **105,** 499–508
33. Ding, S.-Y., Xu, Q., Ali, M. K., Baker, J. O., Bayer, E. A., Barak, Y., Lamed, R., Sugiyama, J., Rumbles, G., and Himmel, M. E. (2006) Versatile derivatives of carbohydrate-binding modules for imaging of complex carbohydrates approaching the molecular level of resolution. *BioTechniques* **41,** 435–436, 438, 440, passim
34. Karlsson, J., Saloheimo, M., Siika-Aho, M., Tenkanen, M., Penttilä, M., and Tjerneld, F. (2001) Homologous expression and characterization of Cel61A (EG IV) of *Trichoderma reesei*. *Eur. J. Biochem.* **268,** 6498–6507
35. Ong, E., Gilkes, N. R., Miller, R. C., Jr., Warren, R. A., and Kilburn, D. G. (1993) The cellulose-binding domain (CBD_{Cex}) of an exoglucanase from *Cellulomonas fimi*: production in *Escherichia coli* and characterization of the polypeptide. *Biotechnol. Bioeng.* **42,** 401–409
36. Tu, M., Chandra, R. P., and Saddler, J. N. (2007) Recycling cellulases during the hydrolysis of steam exploded and ethanol pretreated lodgepole pine. *Biotechnol. Prog.* **23,** 1130–1137
37. Arantes, V., and Saddler, J. N. (2011) Cellulose accessibility limits the effectiveness of minimum cellulase loading on the efficient hydrolysis of pretreated lignocellulosic substrates. *Biotechnol. Biofuels.* **4,** 3
38. Berlin, A., Maximenko, V., Bura, R., Kang, K.-Y., Gilkes, N., and Saddler, J. (2006) A rapid microassay to evaluate enzymatic hydrolysis of lignocellulosic substrates. *Biotechnol. Bioeng.* **93,** 880–886
39. Berezin, I. V., Rabinovich, M. L., and Sinitsyn, A. P. (1977) [Applicability of quantitative kinetic spectrophotometric method for glucose determination]. *Biokhimiia* **42,** 1631–1636
40. Starcher, B. (2001) A ninhydrin-based assay to quantitate the total protein content of tissue samples. *Anal. Biochem.* **292,** 125–129
41. Nishiyama, Y., Langan, P., and Chanzy, H. (2002) Crystal structure and hydrogen-bonding system in cellulose Iβ from synchrotron X-ray and neutron fiber diffraction. *J. Am. Chem. Soc.* **124,** 9074–9082
42. Clarke, K., Li, X., and Li, K. (2011) The mechanism of fiber cutting during enzymatic hydrolysis of wood biomass. *Biomass Bioenergy* **35,** 3943–3950
43. Tozzi, E. J., McCarthy, M. J., Lavenson, D. M., Cardona, M., Powell, L. R., Karuna, N., McCarthy, M. J., and Jeoh, T. (2014) Effect of fiber structure on yield stress during enzymatic conversion of cellulose. *AIChE J.* **60,** 1582–1590
44. Del Rio, L. F., Chandra, R. P., and Saddler, J. N. (2012) Fibre size does not appear to influence the ease of enzymatic hydrolysis of organosolv-pretreated softwoods. *Bioresour. Technol.* **107,** 235–242
45. Gao, S., You, C., Renneckar, S., Bao, J., and Zhang, Y.-H. P. (2014) New insights into enzymatic hydrolysis of heterogeneous cellulose by using carbohydrate-binding module 3 containing GFP and carbohydrate-binding module 17 containing CFP. *Biotechnol. Biofuels.* **7,** 24
46. Arantes, V., Gourlay, K., and Saddler, J. N. (2014) The enzymatic hydrolysis of pretreated pulp fibers predominantly involves "peeling/erosion" modes of action. *Biotechnol. Biofuels* **7,** 87
47. Du, R., Huang, R., Su, R., Zhang, M., Wang, M., Yang, J., Qi, W., and He, Z. (2013) Enzymatic hydrolysis of lignocellulose: SEC-MALLS analysis and reaction mechanism. *RSC Adv.* **3,** 1871
48. Fox, J. M., Jess, P., Jambusaria, R. B., Moo, G. M., Liphardt, J., Clark, D. S., and Blanch, H. W. (2013) A single-molecule analysis reveals morphological targets for cellulase synergy. *Nat. Chem. Biol.* **9,** 356–361
49. Hildén, L., Daniel, G., and Johansson, G. (2003) Use of a fluorescence labelled, carbohydrate-binding module from *Phanerochaete chrysosporium* Cel7D for studying wood cell wall ultrastructure. *Biotechnol. Lett.* **25,** 553–558